

SUPPORTING INFORMATION

Bi₄O(I₃O₁₀)(IO₃)₃(SeO₄): trimeric condensation of IO₄³⁻ monomers into I₃O₁₀⁵⁻ polymeric anion observed in a three-component mixed-anion NLO material†

Fei-Fei Mao,^{a,b} Jin-Yu Hu,^c Bing-Xuan Li^b, and Hua Wu^{*,a}

^a Jiangsu Key Laboratory of Pesticide Sciences, Department of Chemistry, College of Science, Nanjing Agricultural University, Nanjing 210095, P. R. China

^b State Key Laboratory of Structural Chemistry, Fujian Institute of Research on the Structure of Matter, Chinese Academy of Sciences, Fuzhou 350002, P. R. China.

^c Department of Physics, Fuyang Normal University, Fuyang, 236037, P. R. China

SUPPORTING INFORMATION

Table of Contents

Section	Title	Page
Section S1	Materials and Methods	S3-S4
	References	S5
Table S1	Crystallographic Data and structure refinements for $\text{Bi}_4\text{O}(\text{I}_3\text{O}_{10})(\text{IO}_3)_3(\text{SeO}_4)$.	S6
Table S2	Selected bond lengths (\AA) for $\text{Bi}_4\text{O}(\text{I}_3\text{O}_{10})(\text{IO}_3)_3(\text{SeO}_4)$.	S7
Table S3	Calculation of dipole moment (c -component) for IO_3 , SeO_4 , BiO_8 , BiO_7 polyhedra and net dipole moment for a unit cell in $\text{Bi}_4\text{O}(\text{I}_3\text{O}_{10})(\text{IO}_3)_3(\text{SeO}_4)$ ($D = \text{Debyes}$. The direction of c was assumed to be positive.)	S8
Fig. S1	Measured (a) and simulated (b) powder X-ray diffraction patterns of $\text{Bi}_4\text{O}(\text{I}_3\text{O}_{10})(\text{IO}_3)_3(\text{SeO}_4)$.	S9
Fig. S2	The views of Bi_4O_{25} cluster (a), $\text{Bi}(1)\text{O}_8$ and $\text{Bi}(2)\text{O}_7$ polyhedra (b), the stacking mode of the Bi_4O_{25} cluster in $\text{Bi}_4\text{O}(\text{I}_3\text{O}_{10})(\text{IO}_3)_3(\text{SeO}_4)$.	S10
Fig. S3	The views of the coordination mode of the I_3O_{10} (a), IO_3 (b), SeO_4 (c), and the Bi_4O tetrahedron in $\text{Bi}_4\text{O}(\text{I}_3\text{O}_{10})(\text{IO}_3)_3(\text{SeO}_4)$.	S11
Fig. S4	TGA and DSC curves of $\text{Bi}_4\text{O}(\text{I}_3\text{O}_{10})(\text{IO}_3)_3(\text{SeO}_4)$ under a N_2 atmosphere.	S12
Fig. S5	Infrared spectrum of $\text{Bi}_4\text{O}(\text{I}_3\text{O}_{10})(\text{IO}_3)_3(\text{SeO}_4)$.	S13
Fig. S6	UV-vis-NIR absorption spectrum and optical diffuse reflectance spectrum of $\text{Bi}_4\text{O}(\text{I}_3\text{O}_{10})(\text{IO}_3)_3(\text{SeO}_4)$.	S14

Section S1 Materials and Methods

Synthesis.

$\text{Bi}(\text{NO}_3)_3 \cdot 5\text{H}_2\text{O}$ (99+%), I_2O_5 (99.0%), H_2SeO_4 (40+%, AR), and HF (40+%, AR) were used as purchased from Shanghai Reagent Factory. Single crystals of $\text{Bi}_4\text{O}(\text{I}_3\text{O}_{10})(\text{IO}_3)_3(\text{SeO}_4)$ were obtained hydrothermally from a mixture of $\text{Bi}(\text{NO}_3)_3 \cdot 5\text{H}_2\text{O}$ (242.535 mg, 0.5 mmol), I_2O_5 (667 mg, 2 mmol), H_2SeO_4 (400 μL) and 2 mL 10% HF solution in 23 mL Teflon-lined autoclave. The autoclave was heated to 230 °C in 6 h and held for 3 days, and then cooled to 30 °C at a rate of 3 °C/h. Colorless block $\text{Bi}_4\text{O}(\text{I}_3\text{O}_{10})(\text{IO}_3)_3(\text{SeO}_4)$ crystals were collected with a yield of ca. 85% (based on Bi). For the synthesis of the compound, the initial and final reaction media are very acidic (pH<1). Energy-dispersive spectrometry (EDS) elemental analysis on the single-crystals of $\text{Bi}_4\text{O}(\text{I}_3\text{O}_{10})(\text{IO}_3)_3(\text{SeO}_4)$ gave evidence of the existence of Bi, Se, I and O.

Instruments and Methods

Powder X-ray Diffraction.

Powder X-ray diffraction (XRD) patterns were recorded on a Rigaku MiniFlex II diffractometer with graphite-monochromated Cu K α radiation in the 2θ range of 5–65° with a step size of 0.02°.

Energy-dispersive X-ray spectroscopy.

Microprobe elemental analyses and the elemental distribution maps were measured on a field-emission scanning electron microscope (FESEM, JSM6700F) equipped with an energy-dispersive X-ray spectroscopy (EDS, Oxford INCA).

Thermal Analysis.

Thermogravimetric analysis (TGA) and differential scanning calorimetry (DSC) were performed with a NETZCH STA 449F3 unit under a N₂ atmosphere, at a heating rate of 10 °C/min.

Optical Measurements

Infrared (IR) spectra were recorded on a Magna 750 FT-IR spectrometer in the form of KBr pellets in the range from 4000 to 400 cm^{-1} . Ultraviolet–visible–near infrared (UV–vis–NIR) spectra in the range of 200–2400 nm were recorded on a PerkinElmer Lambda 950 UV–vis–NIR spectrophotometer. By using *Kubelka-Munk* function,¹ reflectance spectra were converted into absorption spectra.

Second Harmonic Generation Measurements.

Powder SHG measurements were carried out with Q-switch Nd: YAG laser generating radiations at 1064 nm according to Kurtz and Perry method.² Crystalline samples in the particle-size range of 25-210 μm were used for SHG measurements. For the phase matching experiments, crystalline $\text{Bi}_4\text{O}(\text{I}_3\text{O}_{10})(\text{IO}_3)_3(\text{SeO}_4)$ samples were sieved into distinct particle-size ranges (25-45, 45-53, 53-75, 75-105, 105-150, 150-210 μm). Sieved KDP samples in corresponding particle-size ranges were taken as references for SHG measurements under 1064 nm laser radiation.

Laser Damage Threshold (LDT) Measurements.

The laser-induced damage threshold (LDT) measurements were performed on crystalline samples in the particle-size range of 150-210 μm with AgGaS_2 sample in the same particle-size range as reference, under 1064 nm laser source (10 ns, 1Hz). The laser spot has a diameter of 3.6mm. The energy of the laser emission was gradually increased until the samples turned black in color. It should be noted that the LDT measurement using powder samples is feasible since each crystallite has a diameter much larger than the wavelength of the incident laser. Thus, each crystallite behaves as a macroscopic bulk material with the similar multiphoton absorption (a main process for LDT as the laser pulse width is shorter than 50 ps).³

Single Crystal Structure Determination.

Single-crystal X-ray diffraction data of the title compound were collected on an Agilent Technologies SuperNova dual-wavelength CCD diffractometer with Mo and Cu $K\alpha$ radiation ($\lambda = 0.71073$ and 1.54178 Å) at 293 K. Data reduction was performed with the program *CrysAlisPro*, and absorption correction based on the multi-scan method was applied.⁴ Both structures were solved by direct method and refined by full-matrix least-squares fitting on F^2 using *SHELXL-2014*.⁵ All of the atoms were refined with anisotropic thermal parameters. The structure was checked for missing symmetry elements using *PLATON* and none was found.⁶ The Flack parameter was refined to be $-0.026(9)$ for $\text{Bi}_4\text{O}(\text{I}_3\text{O}_{10})(\text{IO}_3)_3(\text{SeO}_4)$, indicating that the absolute structure is correct.^{7,8} Protons are needed for $\text{Bi}_4\text{O}(\text{I}_3\text{O}_{10})(\text{IO}_3)_3(\text{SeO}_4)$ to achieve charge balance. Crystallographic data and structure refinements of the two compounds are given in Table S1. More details on the crystallographic data for the compound are given in Table S2.

Computational Method.

The structural data of I_3O_{10} was taken from $\text{Bi}_4\text{O}(\text{I}_3\text{O}_{10})(\text{IO}_3)_3(\text{SeO}_4)$ for computation. Electronic frontier orbitals were calculated based on density functional theory (DFT) with the Beck's three-parameter and Lee–Yang–Parr's gradient-corrected correlation hybrid functional (B3LYP) at the 3-21 G level,^{9,10} as implemented in the Gaussian 09 program package.¹¹

References

- 1 P. Kubelka and F. Munk, *Z. Tech. Physical*, 1931, **12**, 886–892.
- 2 S. K. Kutz and T. T. Perry, *J. Appl. Phys.*, 1968, **39**, 3798–3813.
- 3 M. J. Zhang, B. X. Li, B. W. Liu, Y. H. Fan, X. G. Li,; H. Y. Zeng, G. C. Guo, *Dalton Trans* 2013, **42**, 14223–14229.
- 4 R. H. Blessing, *Acta Crystallogr. Sect. A*, 1995, **51**, 33–38.
- 5 G. M. Sheldrick, *Acta Crystallogr. Sect. A*, 2015, **71**, 3–8.
- 6 A. L. Spek, *J. Appl. Crystallogr.*, 2003, **36**, 7–13.
- 7 H. D. Flack, *Acta Crystallogr. Sect. A*, 1983, **39**, 876–881.
- 8 H. D. Flack and G. Bernardinelli, *Chirality*, 2008, **20**, 681–690.
- 9 C. Lee, W. Yang, R. G. Parr, *Phys. Rev. B: Condens. Matter Mater. Phys.* 1988, **37**, 785–789.
- 10 A. D. Becke, *J. Chem. Phys.* 1993, **98**, 5648–5652.
- 11 M. J. Frisch, G. W. Trucks, H. B. Schlegel, G. E. Scuseria, M. A. Robb, J. R. Cheeseman, G. Scalmani, V. Barone, B. Mennucci, K. A. Peterson, H. Nakatsuji, Caricato, M.; X. Li, Gaussian 09, Revision A.02; Gaussian, Inc.: Wallingford, CT, 2009.

Table S1. Crystallographic Data and structure refinements for $\text{Bi}_4\text{O}(\text{I}_3\text{O}_{10})(\text{IO}_3)_3(\text{SeO}_4)$.

formula	$\text{Bi}_4\text{O}(\text{I}_3\text{O}_{10})(\text{IO}_3)_3(\text{SeO}_4)$
Fw	2060.28
crystal system	hexagonal
space group	$R\bar{3}c$
T (K)	293(2)
a (Å)	9.568
b (Å)	9.568
c (Å)	37.542
α (°)	90
β (°)	90
γ (°)	120
V (Å ³)	2998.3(9)
Z	6
λ (Mo-K α) (Å)	0.71073
Dc (g/cm ⁻³)	6.897
μ (mm ⁻¹)	46.661
GOF on F^2	1.097
Flack factor	0.026(9)
R ₁ wR ₂ [$I > 2\sigma(I)$]	0.0464, 0.0959
R ₁ , wR ₂ (all data)	0.0520, 0.0997

$$R_1 = \frac{\sum ||F_o| - |F_c||}{\sum |F_o|}, wR_2 = \left\{ \frac{\sum w[(F_o)^2 - (F_c)^2]^2}{\sum w[(F_o)^2]^2} \right\}^{1/2}.$$

SUPPORTING INFORMATION

Table S2. Important bond lengths (Å) for $\text{Bi}_4\text{O}(\text{I}_3\text{O}_{10})(\text{IO}_3)_3(\text{SeO}_4)$.

$\text{Bi}_4\text{O}(\text{I}_3\text{O}_{10})(\text{IO}_3)_3(\text{SeO}_4)$			
Bi(1)-O(1)	2.38(3)	Se(1)-O(7)	1.61(3)
Bi(1)-O(2)	2.568(10)	Se(1)-O(7)#1	1.61(2)
Bi(1)-O(5)#3	2.38(2)	Se(1)-O(7)#1	1.61(2)
Bi(1)-O(6)#1	2.27(2)	Se(1)-O(4)	1.65(4)
Bi(1)-O(7)	2.47(2)	I(1)-O(1)	1.83(3)
Bi(1)-O(9)#2	2.63(4)	I(1)-O(5)	1.84(3)
Bi(2)-O(8)	2.29(2)	I(1)-O(10)	1.91(3)
Bi(2)-O(8)#1	2.29(2)	I(1)-O(3)	2.355(8)
Bi(2)-O(8)#4	2.29(2)	I(2)-O(6)	1.74(2)
Bi(2)-O(10)	2.49(3)	I(2)-O(8)	1.81(3)
Bi(2)-O(10)#1	2.49(3)	I(2)-O(9)	1.84(2)
Bi(2)-O(10)#4	2.49(3)		

Symmetry transformations used to generate equivalent atoms: #1 -y, x-y, z; #2 -x+y-1, -x-1, z; #3 -x+y-2/3, y-1/3, z+1/6; #4 -x+y, -x, z; #5 -y-1/3, -x-2/3, z-1/6; #6 -y-1, x-y, z; #7 -y-2/3, -x-1/3, z+1/6; #8 -x+y-1/3, y+1/3, z-1/6.

SUPPORTING INFORMATION

Table S3. Calculation of dipole moment (*c*-component) for IO₃, SeO₄, BiO₈, BiO₇ polyhedra and net dipole moment for a unit cell in Bi₄O(I₃O₁₀)(IO₃)₃(SeO₄) (D = Debyes. The direction of *c* was assumed to be positive.)

Bi ₄ O(I ₃ O ₁₀)(IO ₃) ₃ (SeO ₄) (Z = 6)	
Polar unit	Dipole moment (D)
	<i>c</i> -component
IO ₃	16.50
I ₃ O ₁₀	23.92
SeO ₄	1.46
BiO ₈	-2.48
BiO ₇	-3.20
Net dipole moment (a unit cell)	(23.92-3.20)× 2+ (16.50+1.46-2.48) × 6 = 134.32
Dipole moment per unit volume (D·Å ⁻³)	0.045

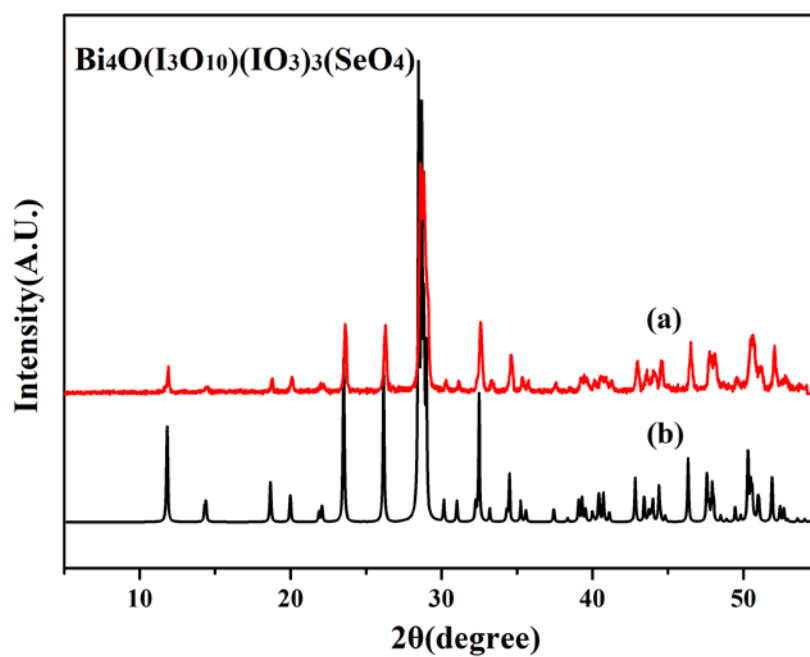


Fig. S1 Measured (a) and simulated (b) powder X-ray diffraction patterns of $\text{Bi}_4\text{O}(\text{I}_3\text{O}_{10})(\text{IO}_3)_3(\text{SeO}_4)$.

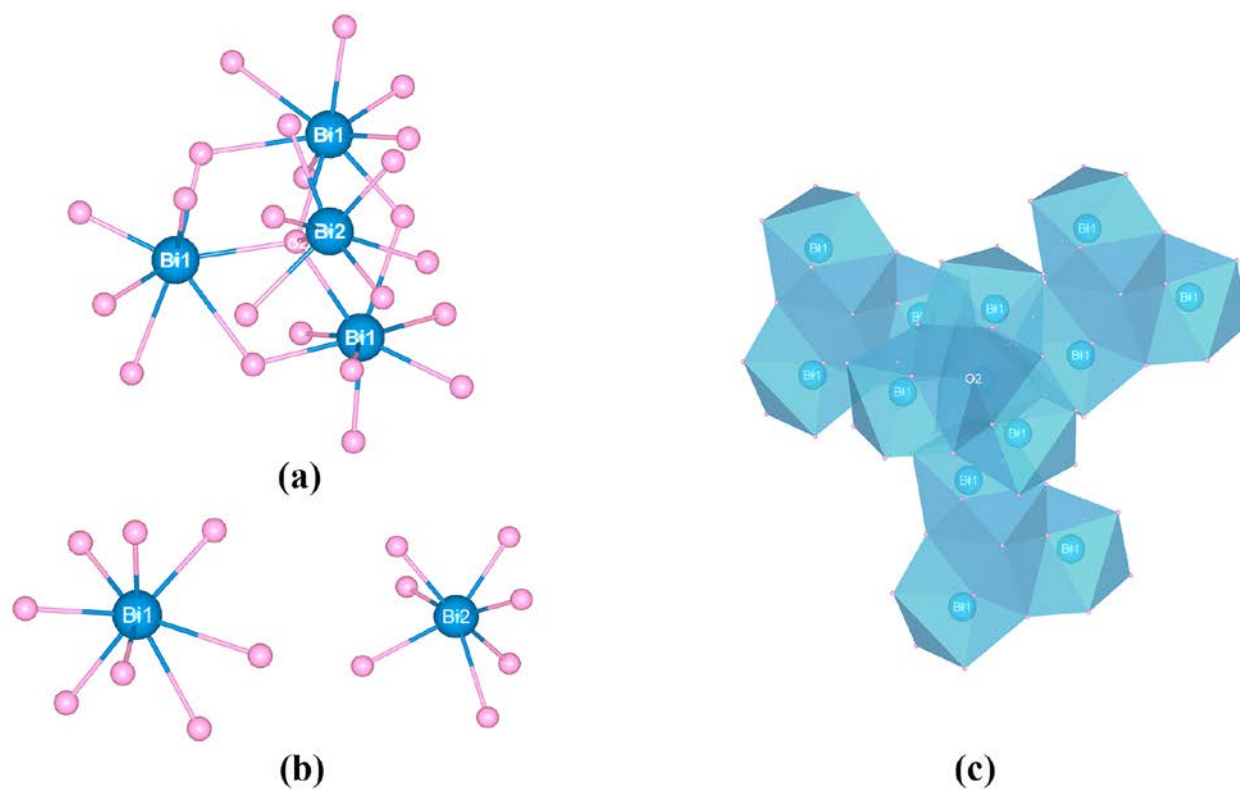


Fig. S2 The views of Bi_4O_{25} cluster (a), $\text{Bi}(1)\text{O}_8$ and $\text{Bi}(2)\text{O}_7$ polyhedra (b), the stacking mode of the Bi_4O_{25} cluster in $\text{Bi}_4\text{O}(\text{I}_3\text{O}_{10})(\text{IO}_3)_3(\text{SeO}_4)$.

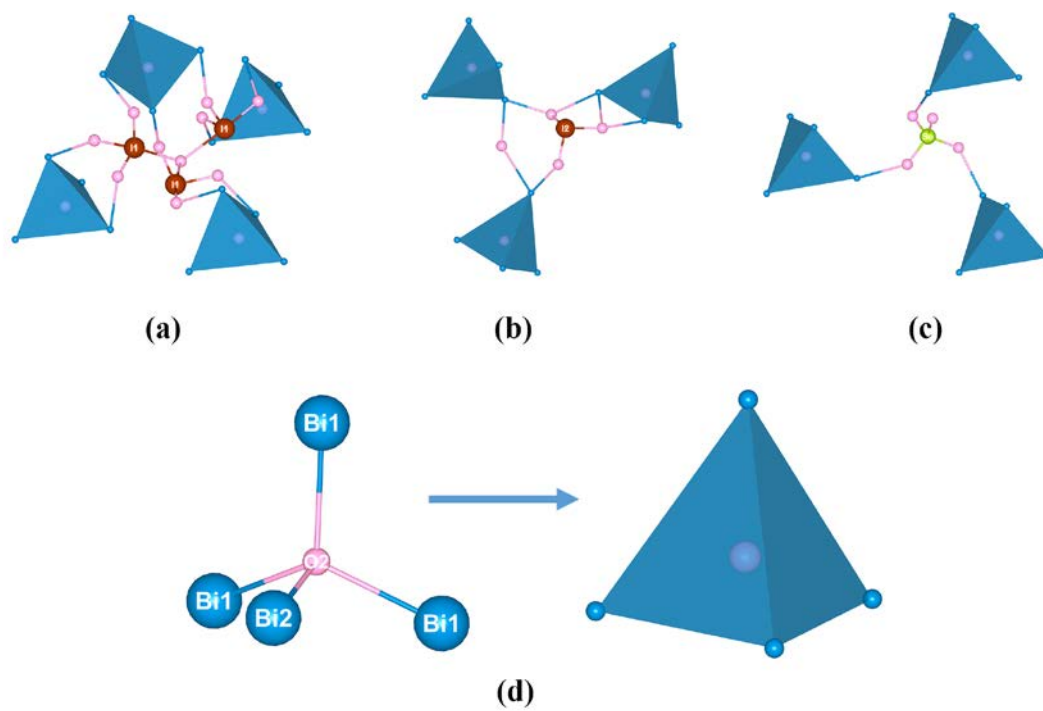


Fig. S3 The views of the coordination mode of the I₃O₁₀ (a), IO₃ (b), SeO₄ (c), and the Bi₄O tetrahedron in Bi₄O(I₃O₁₀)(IO₃)₃(SeO₄).

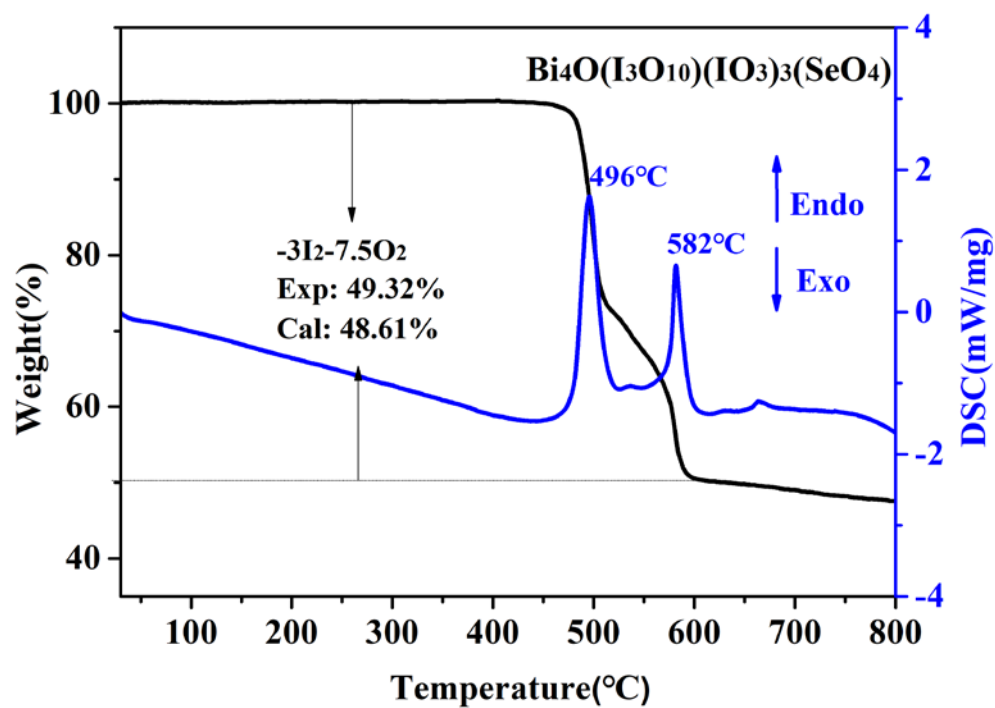


Fig. S4 TGA and DSC curves of $\text{Bi}_4\text{O}(\text{I}_3\text{O}_{10})(\text{IO}_3)_3(\text{SeO}_4)$ under a N_2 atmosphere.

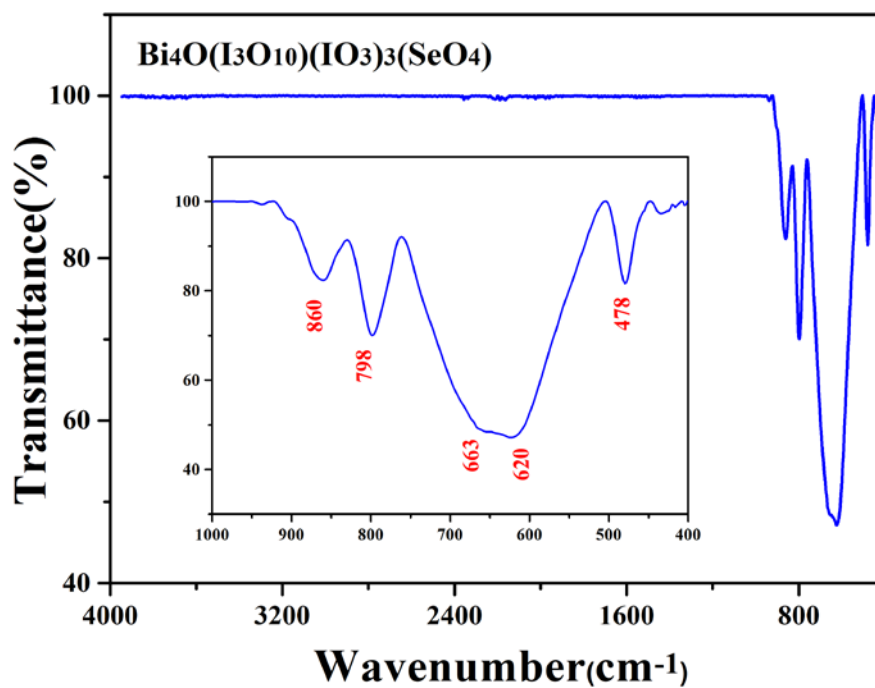


Fig. S5 Infrared spectrum of $\text{Bi}_4\text{O}(\text{I}_3\text{O}_{10})(\text{IO}_3)_3(\text{SeO}_4)$.

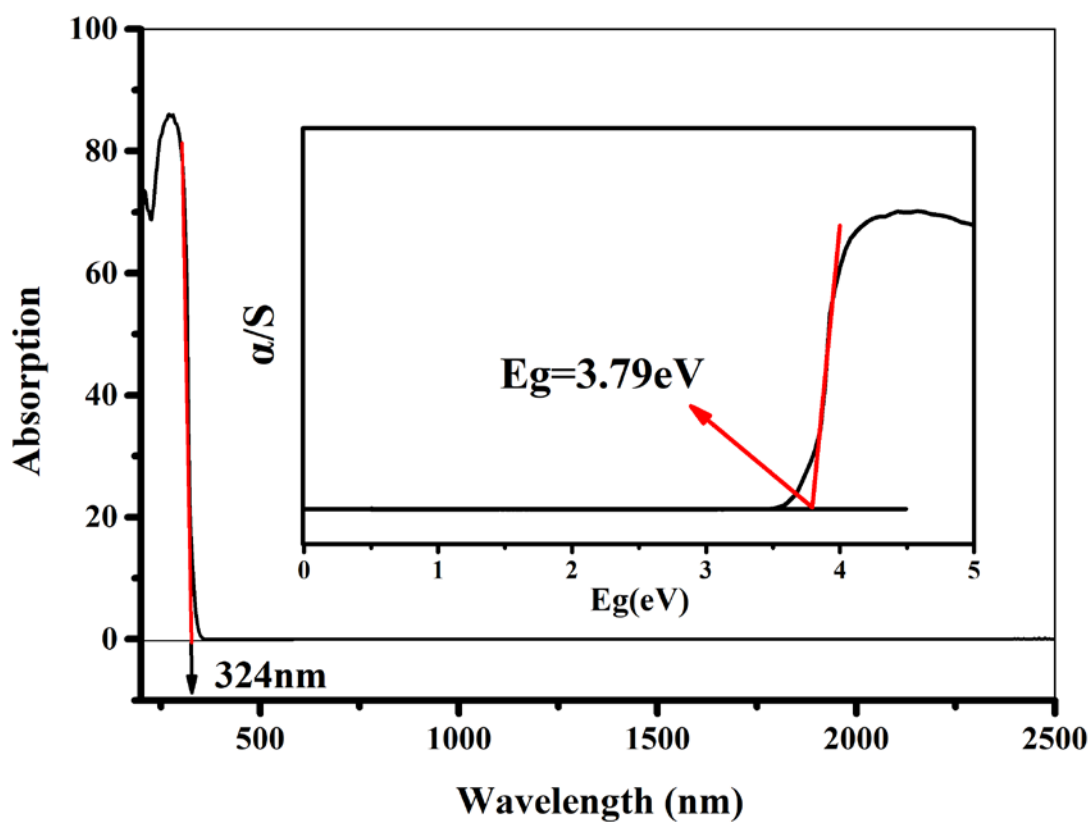


Fig. S6 UV-vis-NIR absorption spectrum and optical diffuse reflectance spectrum of $\text{Bi}_4\text{O}(\text{I}_3\text{O}_{10})(\text{IO}_3)_3(\text{SeO}_4)$.